# Modeling the Impact of Geomagnetically Induced Currents on Electrified Railway Signalling Systems in the United Kingdom

Cameron James Patterson[1], James A. Wild[1], and David H Boteler[2]

[1]Lancaster University
[2]Natural Resources Canada

March 6, 2023

# Modeling the Impact of Geomagnetically Induced Currents on Electrified Railway Signalling Systems in the United Kingdom

**C. J. Patterson[1], J. A. Wild[1], and D. H. Boteler[2]**

[1]Department of Physics, Lancaster University, Lancaster, UK
[2]Natural Resources Canada, Ottawa, Ontario, Canada

**Key Points:**

- A model has been set up to examine geomagnetic effects on DC signalling systems on AC-electrified railways
- Signal misoperations occurred in both modelled UK railway lines when electric fields expected to arise once every 30 years were applied
- Extreme 1 in 100-year geoelectric fields would cause a large number of signal misoperations in both UK railway lines studied

Corresponding author: Cameron Patterson, c.patterson2@lancaster.ac.uk

## Abstract

Studies of space weather impacts on ground-based infrastructure have been largely focused on power networks and pipelines, but railway signalling systems are also affected, with misoperations observed in several countries. This paper advances recent theoretical work on geomagnetically induced currents in railway signalling systems by modeling realistic railway lines with parameters from current industrial standards. Focusing on two example lines in the United Kingdom with different locations and orientation, a range of uniform electric fields are simulated along each modelled line. The results show that misoperations could be caused by geomagnetic interference at disturbance levels expected to recur over timescales of several decades. We also demonstrate that the UK estimate for the geoelectric field induced by a 1 in 100-year extreme storm would be strong enough to cause widespread signal misoperations in both lines studied.

## Plain Language Summary

Naturally occurring geomagnetic disturbances caused by space weather can interfere with technological infrastructure in space and on Earth. Previous measurements show that railways in several countries have been impacted, with geomagnetic interference in signalling systems causing wrong signals to be shown. Signalling misoperations can occur when currents that are induced in the rails by space weather interfere with the preset currents from railway infrastructure used to detect trains. This study demonstrates a model that analyses the impacts of geomagnetic activity on two railway lines in the United Kingdom with different orientation and location. The results show that the signalling systems on both lines are susceptible to misoperations caused by geomagnetic interference with a recurrence timescale of several decades. The UK estimates for a 1 in 100 year extreme storm were strong enough to cause a large number of signal misoperations in both lines.

## 1 Introduction

Space weather poses a risk to infrastructure in space and on the ground. Geomagnetically induced currents (GIC) are one of the foremost space weather hazards. During geomagnetic disturbances, fluctuating ionospheric currents produce changes to the magnetic fields observed at the Earth's surface. As described by Faraday's Law of Induction, this rapidly changing magnetic field drives electric currents in the Earth and through grounded conductors such as power transmission networks (Pirjola, 1985; Boteler, 2014; Lewis et al., 2022), oil and gas pipelines (Pulkkinen et al., 2002; Boteler & Trichtchenko, 2015) and railways (Darch et al., 2014).

A detailed examination of interference from geomagnetic storms in the Swedish railway signalling system was carried out by Alm (1956) and Lejdström and Svensson (1956) where a variety of test cases consisting of different track circuit setups and fault conditions were investigated and suggestions for mitigation provided. An example of railway signalling misoperations due to space weather occurred in Sweden (Wik et al., 2009) during a geomagnetic storm in July 1982, a signal changed from green to red and then reverted to green without the presence of a train in the track section or any other fault conditions. It was later estimated that a geoelectric field of 4-5 V/km was induced as a result of the storm, with the GICs driven through the railway signalling systems explaining the malfunction. Similar occurrences have also been observed in Russia where the statistical correlation between malfunctions and geomagnetic disturbances has been shown (Kasinskii et al., 2007; Ptitsyna et al., 2008; Eroshenko et al., 2010). GICs have also been observed and measured in the electrification systems of the Chinese high-speed railway, including within the track circuits (Liu et al., 2016).

Severe space weather was added to the UK National Risk Register of Civil Emergencies in 2012 (Cabinet Office, 2012). The UK Government's Department for Transport subsequently commissioned a report on rail resilience to space weather with the aim of further understanding the threat that space weather posed to UK railway infrastructure (Darch et al., 2014). This report highlighted the knowledge gaps when it came to track circuit interference, finding that "Signalling assets such as signalling and track circuits are potentially vulnerable to CMEs, and many assets are potentially vulnerable to Single Event Effects" (p. 20). It also identified signalling systems as a potential area of vulnerability, stating "The relative vulnerability of different types of systems (e.g. track-based train detection) is not clear at this stage" (p. 20). In 2015, the "Space Weather and Rail" workshop jointly organised by the European Commission's Joint Research Centre, the Swedish Civil Contingencies Agency, the UK Department for Transport and the US National Oceanic and Atmospheric Administration worked towards furthering understanding of space weather's impacts on railways and raising awareness among operators (Krausmann et al., 2015).

In Section 2 of this paper, we provide an overview of track circuit railway signalling systems and the mechanisms via which they can be impacted by space weather. This work builds upon the theoretical modelling of geomagnetic induction in track circuits presented in Boteler (2021), and in Section 3 we describe the model we have developed for this study. We also provide details on the electrical characteristics of the rails and the track circuit parameters that are included in our model, based on specifications from current United Kingdom industry standards. In Section 4, we introduce the two sections of the UK railway network being studied in this paper. In Section 4.1 we discuss factors that must be considered depending on whether an entire railway line, or only a portion of the line, is being modeled. We also examine which aspects of a railway line's design contribute the most to space weather susceptibility. Finally, in Section 4.2, uniform electric fields are applied to both railway lines included in our investigation and the results discussed, first for a range of realistic values based on geoelectric fields that have led to misoperations in the recent past, then for a 1 in 100-year extreme event.

## 2 Track Circuits

Track circuits are one of the main signalling systems designed to detect trains along a railway line. Figure 1 shows the operational principles of a track circuit on an AC-electrified railway line. Insulated rail joints (IRJs) are spaced along one of the rails (the signalling rail) which separates it into blocks; the other rail (the traction rail) is not broken into sections as it provides the return path for the traction current used to power the train. A voltage source is placed at the start of the block which drives a current through the signalling rail and into a relay at the end of the block, and this current energises the relay which causes a green signal to be displayed, indicating there is no train present, as shown in (a). However, if a train is occupying the block, the wheels and axle redirect the current before it can reach the end, and the relay is not energised leading to a red signal that indicates a train is present, as shown in (b). The lengths of track circuit blocks and the traction rail can vary depending on if the section is located in a rural or an urban area. The two lines investigated in this study had a range of track circuit block lengths from 0.4−1.9 km and traction rail lengths of around 34 km and 76 km; for comparison, values for the Swedish railway studied by Alm (1956) and Lejdström and Svensson (1956) were 1 km and 4 km for track circuit blocks and 100 km for the traction rail.

By design, the normal operation of a track circuit relay requires it to energise or de-energise at specific current thresholds. This balance can be offset by geomagnetically induced currents which can either work to de-energise a relay in a block with no train present causing a 'right side failure' (a mode of failure that does not compromise the safety of trains) or energise a relay in a block with a train present causing a 'wrong side failure' (one which does compromise the safety of trains).

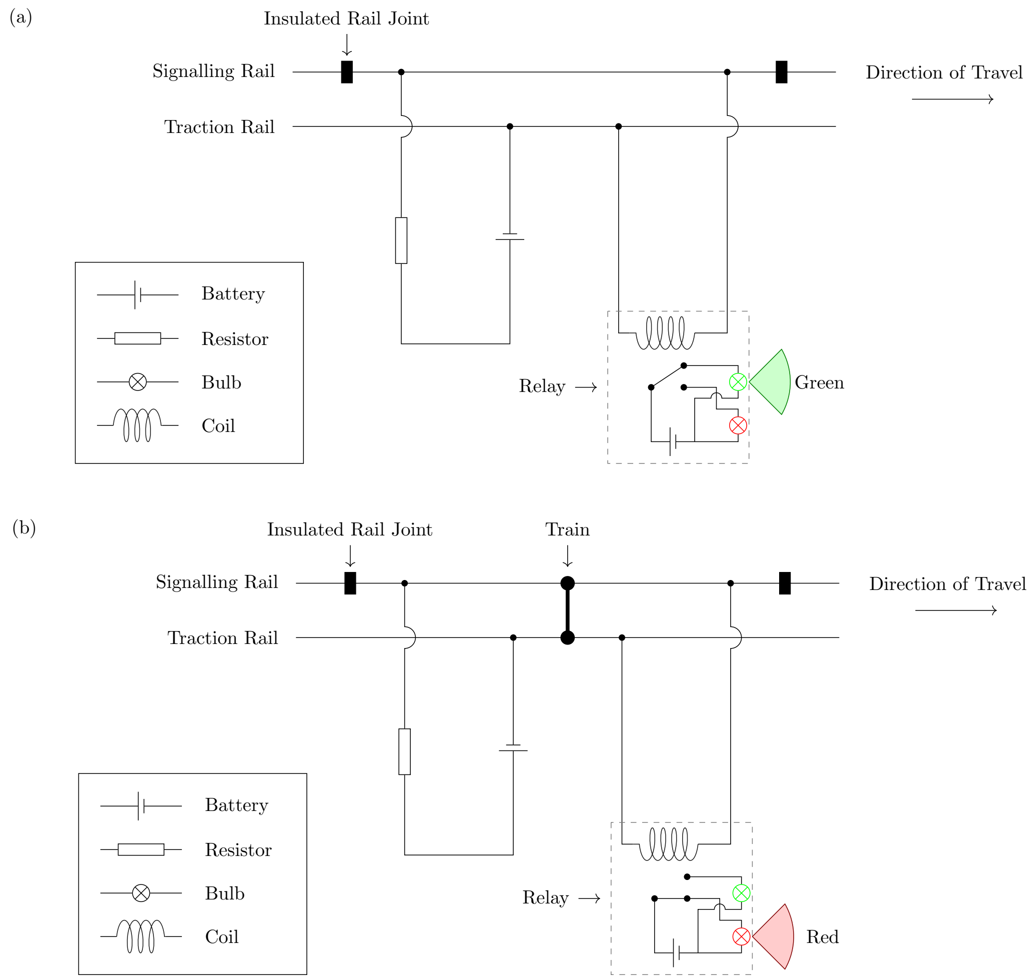


**Figure 1.** Circuit diagram of a railway signalling track circuit for a single block along a network in the cases of (a) the absence of a train in the block and (b) a train occupying the block. Insulated rail joints separate each block from its neighbours, while the continuous rail is connected across all blocks. A power supply is connected to the side of the circuit from which the train enters (left in this case) and an accompanying resistor to protect it from short-circuiting; the relay is on the far end of the block (right in this case), formed of resistors and an electromagnet which in (a) is energised by the power supply, causing the switch to be in the configuration to display a green light, indicating the section is clear. When a train enters the block, as in (b), the wheels and axle short circuit the power supply causing the electromagnet to be de-energised, and the switch falls to the configuration that displays a red light, indicating the section is occupied.

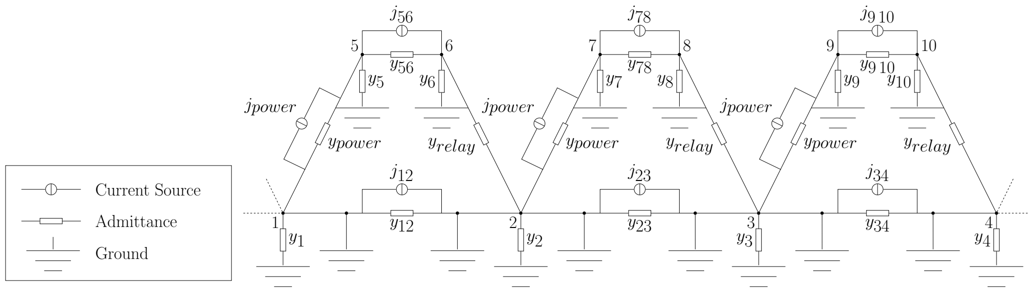


**Figure 2.** Circuit diagram showing the nodal admittance network of three track circuits separated by insulated rail joints and connected by the traction rail. The components making up the network are the current source and admittance of the power supply ($j_{power}$ and $y_{power}$ respectively), the admittance of the relay ($y_{relay}$), the admittance to the ground at each node (e.g., $y_1$, $y_2$), the admittance due to the rail between nodes, (e.g., $y_{12}$, $y_{23}$), and the currents induced in the rails due to the geoelectric field between nodes (e.g., $j_{12}$, $j_{23}$).

# 3 Constructing the Network

## 3.1 Geomagnetic Induction Modeling

The analysis in this paper builds upon modeling techniques for geomagnetic induction in track circuits developed by Boteler (2021) and references therein. Each rail is considered to be a transmission line with series impedances and parallel admittances equivalent to the resistance of the rails and the leakages to the ground respectively. The transmission line model for each rail is then converted to an equivalent-pi circuit constructed with admittances and current sources (Boteler, 2013), and the circuits for both rails are combined with the track circuit relay components to form a nodal admittance network, as shown in Figure 2. By design, the traction rail is also periodically connected to the earth to avoid hazardous voltage build-ups, and these grounding points are also included at this stage.

The power supply current sources, $I_{power}$, are calculated using Equation 1, where $V_{power}$ is the power supply voltage and $r_{power}$ is the power supply resistance.

$$I_{power} = \frac{V_{power}}{r_{power}} \tag{1}$$

The current sources induced as a result of the electric field are calculated with Equation 2, where $E_{\parallel}$ is the electric field component parallel to the rail and $Z$ is the series impedance of the rail.

$$I_E = \frac{E_{\parallel}}{Z} \tag{2}$$

The sum of current sources directed into each node is combined to form $[J]$ (a matrix of nodal current sources). Equation 3 shows the relationship between $[J]$, the voltages at each node ($[V]$), and the network admittances ($[Y]$). In $[Y]$ the diagonal terms are equal to the sum of all admittances connected to that node, the off-diagonal terms are given by the negative of the admittance between nodes, and $[V]$ is the voltage at each node.

$$[J] = [Y][V] \tag{3}$$

The nodal voltages can be obtained by inverting the matrix $[Y]$ and multiplying by the nodal current sources $[J]$, as shown in Equation 4. The difference between two nodal voltages on either side of the relay gives the potential difference across the relay, and thereafter the current flowing across the relay can be calculated.

$$[V] = [Y]^{-1}[J] \tag{4}$$

### 3.2 Rail and Track Circuit Properties

Obtaining realistic values for the electrical characteristics of an AC railway network is crucial to analysing the impacts of GICs in DC signalling systems to the best degree of accuracy. The sections of track considered in this paper are 2-track with single-rail return and no earth wires, where 2-track means that there are two pairs of rails side-by-side, one for each direction of travel.

#### *3.2.1 Rail resistance*

The railway lines being modelled use UIC 60 ($60\,\mathrm{kg\,m^{-1}}$) rail (NR/GN/ELP/27312, 2006), the dimensions are provided by *British Steel: Rail Product Range* (2020) from which a cross-section area of $7600\,\mathrm{mm^2}$ was calculated. We have used a value of $220\,\mathrm{n\Omega\,m}$ for the resistivity of British Steel Grade 700 steel giving a resistance per unit length of the rail as $0.0289\,\Omega\,\mathrm{km^{-1}}$. Mariscotti (2020) and sources therein provide the same value for the per unit length resistance of UIC 60 rail.

#### *3.2.2 Earthing and bonding*

The traction rail itself is not entirely continuous since track geometry or safety design features will call for occasional gaps or side switching. In such cases, both sides of each break in the rail are bonded together to ensure a continuous path for traction return current to flow. Figure 3 illustrates some of the cases where bonding is needed. These include, but are not limited to, continuity bonds used to bridge expansion joints (designed to account for the thermal expansion that rails experience with seasonal temperature changes), cross bonds (used to connect all traction rails on a line together with a path to ground to ensure low impedance is maintained throughout the line) and transposition bonds (used when the traction rail switches sides). The latter requirement can arise in numerous circumstances, including at turnouts (junctions) where they are needed to avoid the short-circuiting of adjacent track circuits. The traction rail is also bonded to all of the overhead line equipment (OLE) structures, in particular the masts located approximately every 60 m along the rail. The mast foundations connect the whole system to Earth, contributing significantly to the leakage to ground from the traction rail (Keenor, 2021).

#### *3.2.3 Leakage admittance*

The leakage admittance of a rail is determined by the rail fastenings, sleepers (crossties) and the ballast, and varies over a wide range due to environmental conditions and underlying ground. NR/GN/ELP/27312 (2006) gives the conventional figure for leakage admittance used by Network Rail to be $0.125\,\mathrm{S\,km^{-1}}$, however, the configuration of the rails means that the signalling and traction rails have different leakage admittance. The signalling rails have insulating pads that reduce leakage, giving a leakage admittance of $0.1\,\mathrm{S\,km^{-1}}$; the traction rails are bonded to OLE structures, this results in a much larger leakage admittance of $1.6\,\mathrm{S\,km^{-1}}$. Another factor considered in this study is the additional leakage from earth mats bonded to the traction return circuit at traction feeder

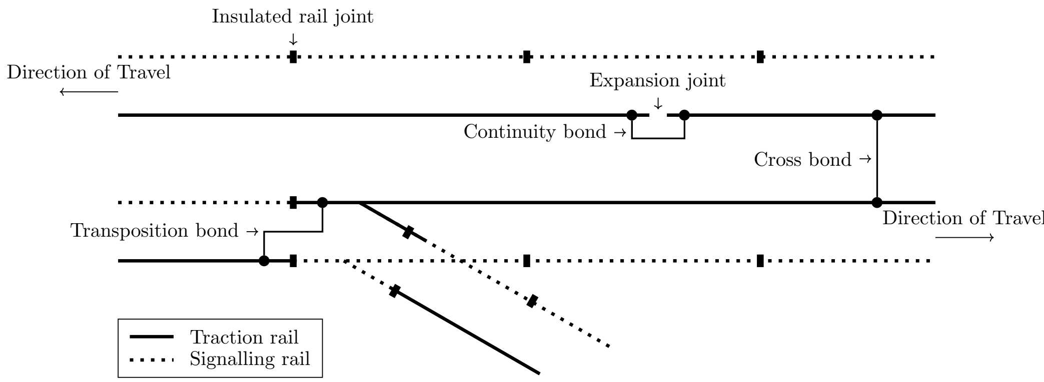


**Figure 3.** A schematic diagram showing the usage of the various bonds required to ensure a continuous path for the current is provided in the traction rail. Along the top traction rail, a continuity bond is used to bridge the gap over an expansion joint designed to protect rails from the effects of thermal expansion during seasonal temperature changes; along the bottom traction rail, transposition bonds are used to temporarily switch the sides of the traction rail due to a turnout (junction) to avoid short-circuiting the track circuit in the branch; connecting both traction rails is a cross bond, designed to ensure voltages are evenly spread across all rails in a line to decrease the hazard of unsafe voltages building up along a rail.

stations, these structures increase the leakage by 10 S for each feeder station (NR/SP/SIG/50004, 2006). In the lines examined in this study, a feeder station is located between Preston and Lancaster.

#### *3.2.4 Track circuits*

Track circuit parameters, including power supply and relay components, vary across the world and even within a specific country, with many different types of equipment and configurations being used. For the UK lines, we obtained the relevant data from the Network Rail Standards Portal. In this study, we have used the combination of 'BR867 AC Immune DC Track Feed Unit' (NR/BR/867, 1990) and the 'BR939A Miniature Tractive Armature AC Immune DC Neutral Track Relay' (NR/BR/939A, 1971). This represents the preferred design according to the most recent Network Rail standards (NR/PS/SIG/11755, 2000). The side of the track circuit from where the train enters consists of a 10 V power supply in series with a 7.2 Ω resistor to limit the current when short-circuited by the locomotive, the far end consists of the relay coil with a resistance of 20 Ω. The pickup current of the relay is 0.081 A with the dropout current being 68 per cent of that value at 0.055 A, this means when the current flowing through an energised relay drops below 0.055 A, the relay will be de-energised and for it to be energised again, the current will need to exceed 0.081 A.

## 4 Results

### 4.1 Railway Line Modeling

The geographical data for the railway lines studied, i.e., the longitudes and latitudes of points along the line were obtained from OpenStreetMap. The lengths of track circuit blocks and hence their start and end points were estimated using Network Rail Sectional Appendices and the railway tracking website Traksy (https://traksy.uk/live). Once the lines were separated into blocks, the orientation of each block in the line was

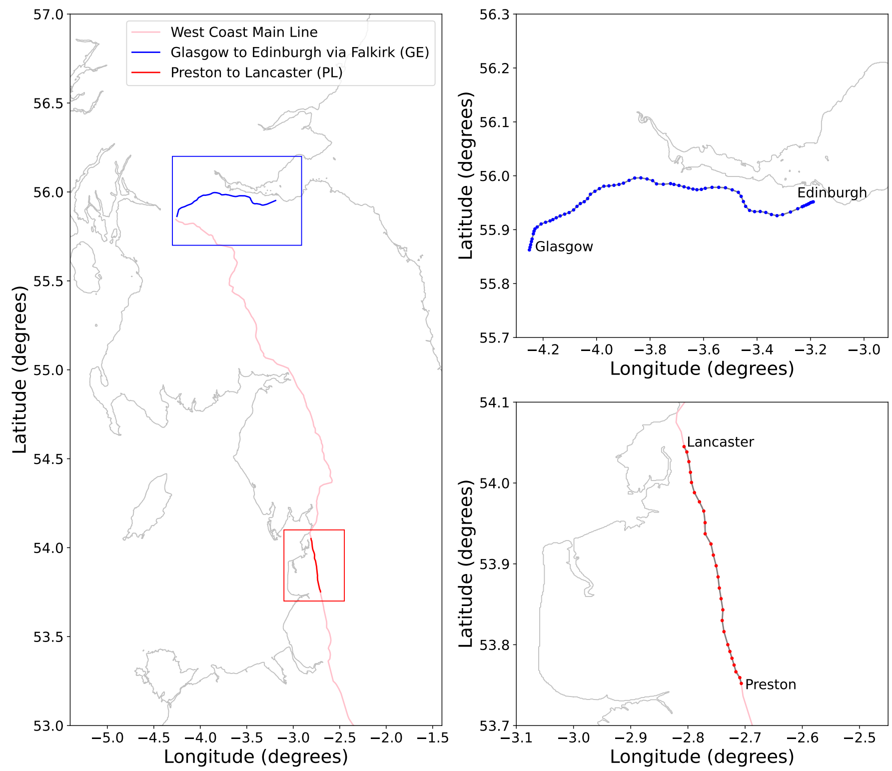


**Figure 4.** A geographic map of a northern portion of the United Kingdom showing both chosen railway lines for study in this paper with areas of interest highlighted and enhanced (top right and bottom right) to show the locations of signals. The top line (blue) is the Glasgow to Edinburgh via Falkirk line, stretching in an east-west orientation; the bottom line (red) is a portion of the West Coast Main Line from Preston to Lancaster, with the extension beyond those sections displayed opaquely, stretching in a north-south orientation.

calculated and used to determine the parallel electric field component along each line segment.

The sections of the railway network chosen for this study are introduced in Figure 4: the 76 km Glasgow to Edinburgh via Falkirk line and a 34 km portion of the West Coast Main Line from Preston to Lancaster. Both lines are electrified with 50 Hz AC at 25 kV. The two sections were selected for their different orientation (east-west for Glasgow to Edinburgh and north-south for Preston to Lancaster) and different geological terrane. For the following analyses, we will consider only the track in one direction of travel, eastwards for Glasgow to Edinburgh and northwards for Preston to Lancaster. Each track circuit is assumed to consist of one power supply at the start of the block (relative to the direction of travel) and one relay at the end of the block.

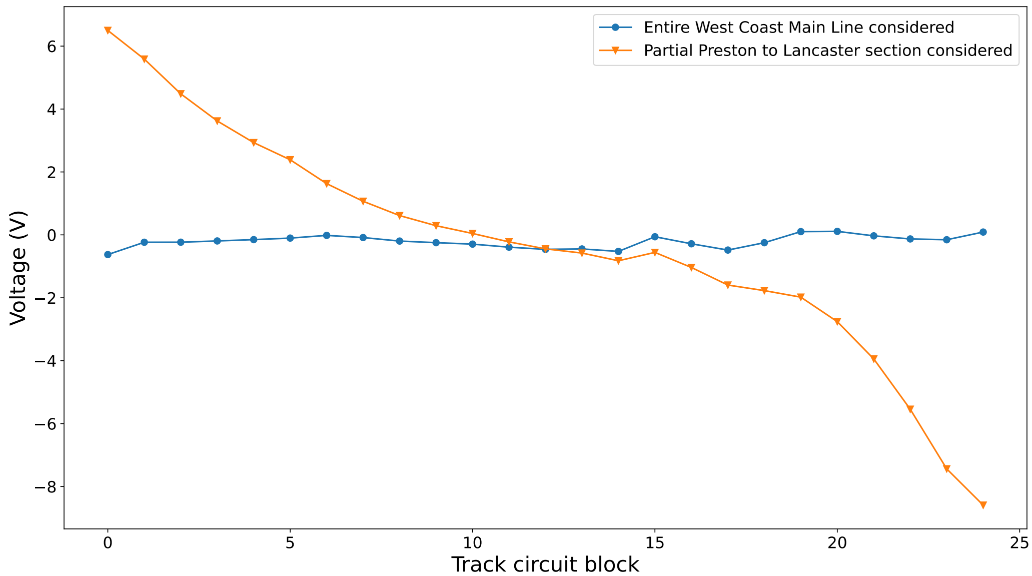


**Figure 5.** The voltage profiles along the traction rail between Preston and Lancaster with different termination conditions. The orange line with triangles shows the voltage profile where the traction rail ends have been set at Preston and Lancaster; the blue line with dots shows the profile where the traction rail has been extended with 310×1 km blocks south of Preston and 230×1 km blocks north of Lancaster with orientations representative of the general line geometry to account for the portions of the West Coast Main Line beyond the area of study.

#### *4.1.1 Modeling a Section of a Line*

When modeling track circuits within a section of traction rail that extends beyond the area of study such as the Preston to Lancaster segment of the West Coast Main Line (WCML), the entire length of the rail must be represented in the model to provide a valid voltage profile along the traction rail section and accurate current values across the relays. To more accurately model the geomagnetic interference on the Preston to Lancaster section, 310×1 km blocks before the section and 230×1 km blocks after the section have been included in the model, with orientation representative of the general line geometry of the WCML. The Preston to Lancaster section of the line still uses the original estimated block lengths, which range from 0.6−1.8 km. Figure 5 compares the voltage profiles along the section of traction rail between Preston and Lancaster when (1) the ends of the traction rail are set at Preston and Lancaster and (2) the ends of the traction rail are extended to encompass the entire WCML using the method detailed above. It can be seen that the voltage profile is significantly different if the entire length of the traction rail is not considered. If detailed information about the adjacent rail sections is not available, but the adjacent rails are uniform and nearly straight, they can be represented by an equivalent 'active termination' (Boteler, 1997) where the external portion of the rail is a single voltage source and series resistance connected to ground. Calculations with active terminations to represent the northern and southern sections of the WCML give almost identical results to those from calculations including the additional representative sections beyond the area of study.

#### *4.1.2 Modeling the Entire Line*

The methodology described above is suitable for analysing portions of lines that do not include either or both ends of the traction rail. But additional considerations have to be made when modeling the entire traction rail due to the effects of the ends of the line. To demonstrate this, a simplified track circuit model has been produced, consisting of 70×1 km blocks all orientated directly eastwards. The track circuit voltage has been set to zero, allowing us to examine the effects of only the induced currents. Figure 6 shows the voltage profiles and nodal voltages along the traction rail and each of the signalling rails when eastward electric fields of $-2\,\mathrm{V\,km^{-1}}$ and $-4\,\mathrm{V\,km^{-1}}$ were applied. The short thin lines illustrate how rail voltage is neither constant from node-to-node nor continuous across nodes. The potential differences across the relays in each track circuit block are shown in a separate panel. The voltage profiles along the traction rail and signalling rails agree with the characteristic electrically long and electrically short profiles as shown in Boteler (2021), respectively. It can be seen that with a constant uniform electric field applied, the nodal voltages of the traction rail and signalling rails, although having different minima and maxima, decrease along the line, following a sideways S-shaped curve. At the beginning of the line, the voltages start at their maximum point, decreasing to a central plateau. At a point near the termination of the line, the nodal voltages of both rails converge, causing the potential difference across the relay to be zero. Closer to the termination of the line the polarity of the potential difference is reversed. It can also be seen that the location of the crossover point where the potential difference reverses remains constant regardless of the electric field strength applied. In Figure 7, the crossover point can be seen at track circuit block 64, and beyond that point the polarity of the currents is reversed.

Considering this from a mathematical point of view: from Equation 4 we know that the nodal voltages are the result of matrix multiplication between the inverse of the admittance matrix ($[Y]^{-1}$) and the current sources ($[J]$). When we increase or decrease the electric field strength ($E$), we are only changing the values of $[J]$, as $[Y]$ is determined by the electrical characteristics of the rails and the track circuit components. $[J]$ is proportional to $E$ and inversely proportional to the rail impedance. However, as the impedances of the signalling rails and traction rail are equal, changing $E$ scales the currents induced in all rails by the same factor. As $[Y]^{-1}$ is constant and $[J]$ has been scaled by a certain factor, the result of the matrix multiplication is that $[V]$ would be scaled by the same factor. The current across the relays is determined by the relay resistance, which is constant, and the potential difference across the rail, which is the difference between two voltage nodes within $[V]$. This means that the potential difference is again scaled by that same factor. Consequently, when the potential difference is zero, scaling it by any factor would still result in zero, leading to a common crossover point that is independent of the electric field strength.

#### *4.1.3 Susceptibility to Geomagnetic Interference*

In this section, we investigate the factors which contribute to the susceptibility of a track circuit relay to induced currents. For the Glasgow to Edinburgh line, the model was run for eastwards electric field values of 0 to $-4\,\mathrm{V\,km^{-1}}$ in increments of 0.1, recording the current across the relay in each block for every E-field value. The blocks were then sorted by length and the range of currents across each relay was plotted to determine if there was a dependence on block length. To examine the effects of the angle between a block's rails and the geoelectric field, a second set of modelled data was taken with the E-field in each block orientated along the rail. The results of this modeling are shown in Figure 8. Due to the effects of the ends of the traction rail on the voltage profiles, we split the blocks near the ends from those in the centre. When compared with blocks of similar length in the centre of the line, the range of current values across relays towards the ends of the line is larger near the start and smaller and oppositely di-

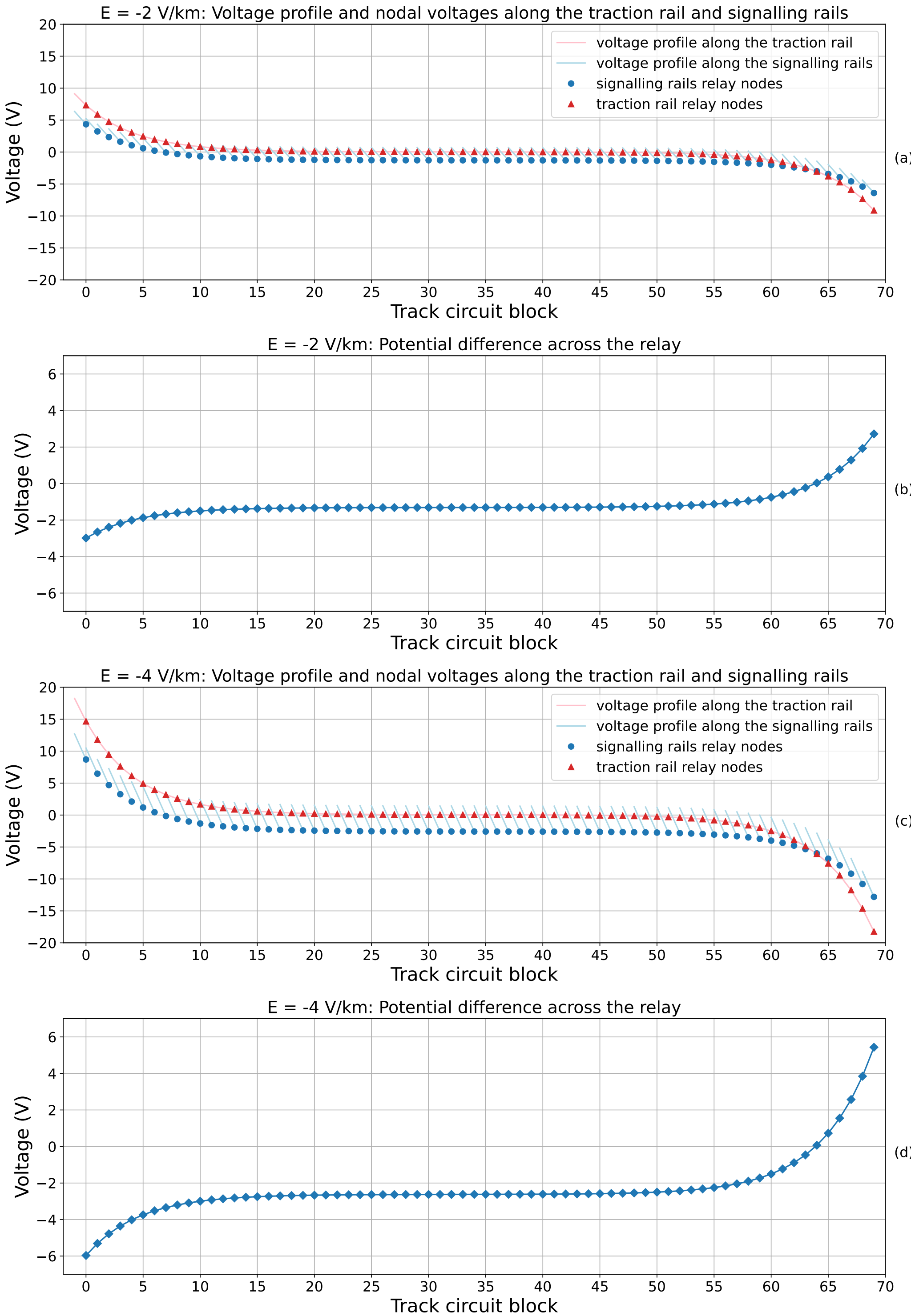


**Figure 6.** Parameters in a network of $70 \times 1$ km blocks facing directly eastwards, where the track circuit voltage is set to zero. For electric field strengths of $-2\,\mathrm{V\,km^{-1}}$: panel (a) shows the voltage profiles and nodal voltages along the traction rail (red triangles) and signalling rails (blue dots) and panel (b) shows the potential difference across the relays along the line (blue diamonds). The point at which the signalling rail voltage and traction rail voltage are equal and hence the point at which the potential difference is zero occurs at the same location regardless of electric field strength. Panels (c) and (d) are the equivalent of (a) and (b) but for $-4\,\mathrm{V\,km^{-1}}$.

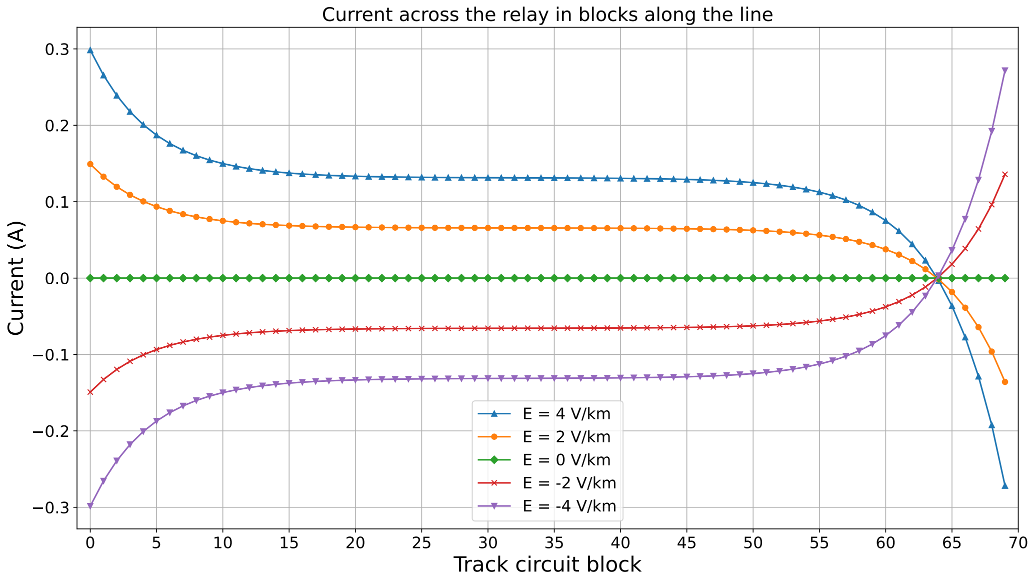


**Figure 7.** Parameters in a network of $70 \times 1$ km blocks facing directly eastwards, where the track circuit voltage is set to zero: the current across the relays along the line for electric field strengths ranging from $4\,\mathrm{V\,km^{-1}}$ to $-4\,\mathrm{V\,km^{-1}}$. Independent of electric field strength, the currents cross zero at a common point.

rected near the termination. The angle between the E-field and the rails has a definite impact, the currents induced in the section will be largest when the E-field is parallel to the rail and zero when the E-field is perpendicular to the rail. Most of the rails in blocks between Glasgow and Edinburgh are closely aligned with the direction of the E-field so the currents through most of the relays experience only minor variation, the exceptions we see are mainly due to the northwards orientation of the track leaving Glasgow before turning east towards Edinburgh. If we consider only blocks at the centre of the line, the length of the blocks is a first-order indicator of the current through the relay. Considering the case when the E-field is aligned with the rails (shown by blue dashed lines in Figure 8), relay misoperations occur where the blocks are the longest. Other subtle effects can also be noted, i.e., the length of surrounding blocks, which affects the current across the relay of a block in between. This analysis was repeated for Preston to Lancaster with a northwards electric field without the need to filter blocks near the ends due to it being a central segment of the West Coast Main Line. The results, as shown in Figure 9, agree with those for Glasgow to Edinburgh, i.e., the longer blocks are more susceptible to geomagnetic interference than shorter ones.

## 4.2 Applying Electric Fields

### *4.2.1 Uniform Electric Fields*

For the following analysis, a range of uniform electric field values between $\pm 4\,\mathrm{V\,km^{-1}}$ have been applied. They are based on the lower limit of geoelectric field values observed in Sweden during the storm of July 1982, where interference on railway signalling was observed (Wik et al., 2009). Each block is assumed to be absent of any trains meaning all signals should displaying a green light, with the current flowing through the relay at a value above the relay dropout threshold.

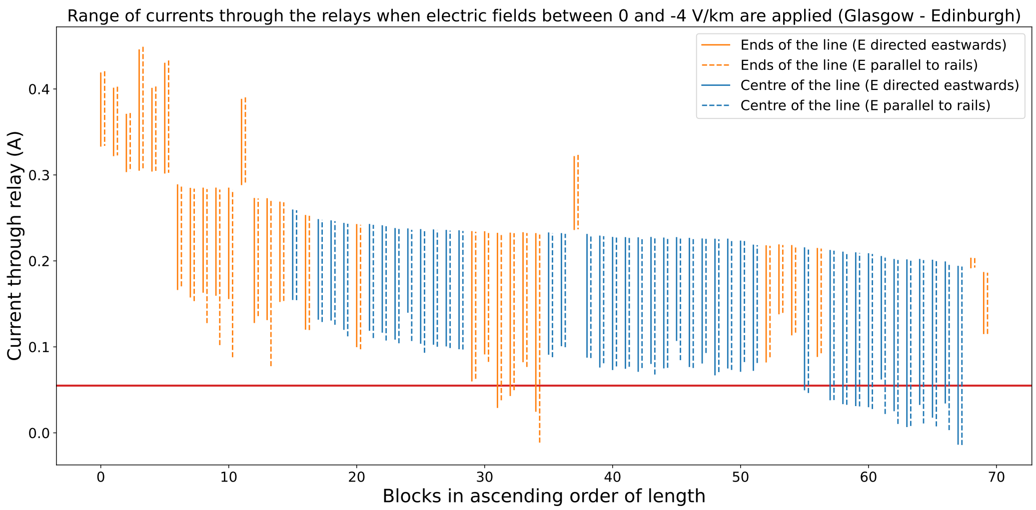


**Figure 8.** The range of currents across each relay in blocks along the line between Glasgow and Edinburgh for electric fields between 0 and $-4\,\mathrm{V\,km^{-1}}$. Solid lines show the results for when there is an angular separation between the rails and the electric field, and the dashed lines show the results for when the electric field is parallel to the rails in each block. Blocks at the centre of the rail are shown as blue lines and blocks at the ends as orange lines. The horizontal red line indicates the threshold below which the track circuit would de-energise.

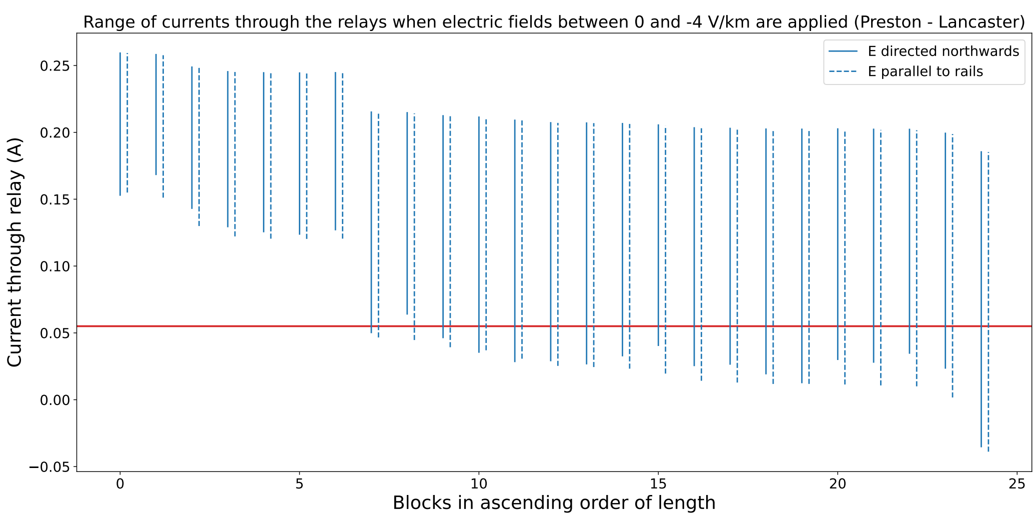


**Figure 9.** The range of currents across each relay in blocks along the line between Preston and Lancaster for electric fields between 0 and $-4\,\mathrm{V\,km^{-1}}$. Solid lines show the results for when there is an angular separation between the rails and the electric field, and dashed lines show the results for when the electric field is parallel to the rails in each block. The horizontal red line indicates the threshold below which the track circuit would de-energise.

Figure 10 shows the current through the relay of each track circuit block along the two sections assuming no external electric field is applied, the line below each main panel is a schematic representation of all the signals along the section where a green outline with no fill indicates normal operation and black outline with red fill indicates a false signal. It can be seen that all relays are operating normally, with the differences in current arising from network design factors such as the length of blocks and the inclusion of traction feeder stations.

Assuming the field is uniform across the entire area of the section, electric fields ranging from 4 to $-4\,\mathrm{V\,km^{-1}}$ increasing in intervals of $0.1\,\mathrm{V\,km^{-1}}$ were applied. For the "east-west" orientated Glasgow to Edinburgh line, the electric field was aligned to geographic east ($E_y$). For the "north-south" orientated Preston to Lancaster section, a geographic north direction ($E_x$) was chosen.

For Glasgow to Edinburgh, the threshold westward electric field value at which signal misoperations begin to occur is $E_y = -2.8\,\mathrm{V\,km^{-1}}$. At the most negative electric field ($E_y = -4\,\mathrm{V\,km^{-1}}$) of the range we have applied, the currents induced in the track circuits are sufficiently strong to cause 14 of the relays to de-energise, displaying false signals as seen in Figure 11. With Glasgow to Edinburgh, as we are modeling the entire line, it is also important to look at the case of positive (eastward) electric fields due to the reversed potential difference beyond the crossover point. At $E_y = 4\,\mathrm{V\,km^{-1}}$, the de-energisation of the blocks beyond the crossover can be seen in Figure 12 when compared with the profiles of the negative electric fields. However, no signal misoperations occur due to the short length of the blocks towards the termination of the line.

For Preston to Lancaster, the threshold southward electric field value at which signal misoperations begin to occur is $E_x = -2.5\,\mathrm{V\,km^{-1}}$. At $E_x = -4\,\mathrm{V\,km^{-1}}$, the currents induced in the track circuits cause 17 of the relays to be de-energised, as seen in Figure 13. As Preston to Lancaster is a central segment of the WCML, positive (northward) electric field values are not considered.

#### *4.2.2 1 in 100 Year Extreme*

An estimate for a 1 in 100-year extreme geoelectric field for the UK is estimated by Beggan et al. (2013) to be approximately $5\,\mathrm{V\,km^{-1}}$. As we are considering an extreme case, we set the value to be negative (opposite to the direction of travel) for both lines being modelled. The currents across the relays for sections A and B are shown in Figures 14 and 15 respectively, with nearly all of the relays being de-energised between Preston to Lancaster and almost half of all relays being de-energised between Glasgow and Edinburgh. This suggests that a 1 in 100-year extreme geoelectric field value applied to the two railway sections would result in significant signal misoperations.

## 5 Discussion

This study expands upon the theoretical work of Alm (1956), Lejdström and Svensson (1956) and Boteler (2021) by modeling realistic railway lines with parameters from current industrial standards. The electrical characteristics and parameters for the rails and track circuit components are specific to the UK 25 kV, 50 Hz AC railway lines, e.g., the West Coast Main Line and the Glasgow to Edinburgh via Falkirk line. These values can be replaced as necessary which allow the modeling to be used for any combination of rails, blocks and relay types, provided the data for those components are available. The main reason we chose a section of the West Coast Main Line was because it is one of the UK's most important railway lines. It provides rail links to major cities, including an arterial connection between England and Scotland. With a pre-pandemic estimate of 35 million passengers annually (Department for Transport, 2015), the West Coast Main Line provides crucial services including local and regional travel as well as

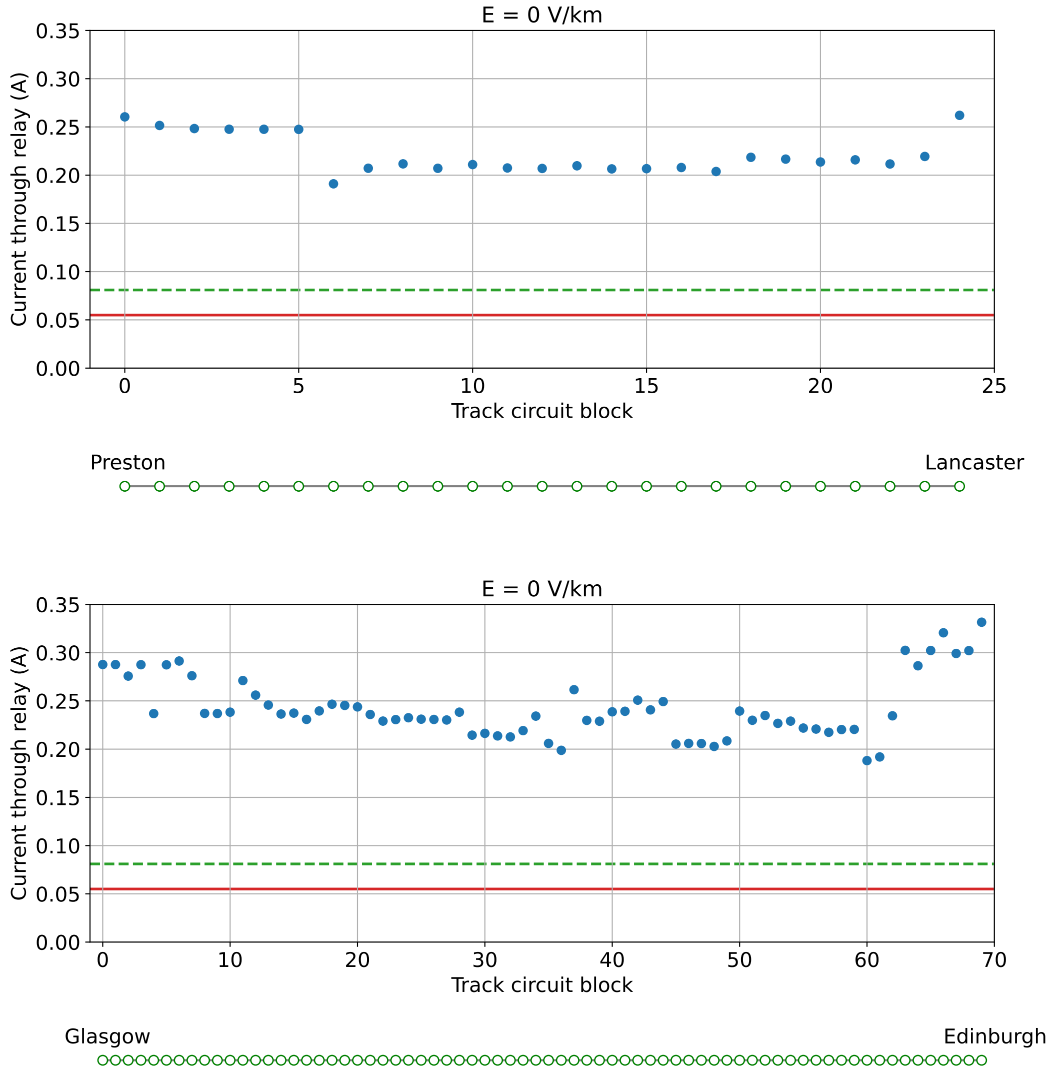


**Figure 10.** In the absence of a train: the current through each of the track circuit relays between Preston and Lancaster (top panel) and Glasgow to Edinburgh (bottom panel) with no geoelectric field applied. The blue dots indicate the current of each relay, the red (solid) line shows the threshold below which the track circuit would de-energise and display an incorrect signal, and the green (dashed) line shows the threshold the current would need to rise above to re-energise if de-energised. Below each plot is a schematic view of each signal and whether it is operating correctly. An unfilled green dot means normal operation, so in this case, all signals on both lines show no misoperations.

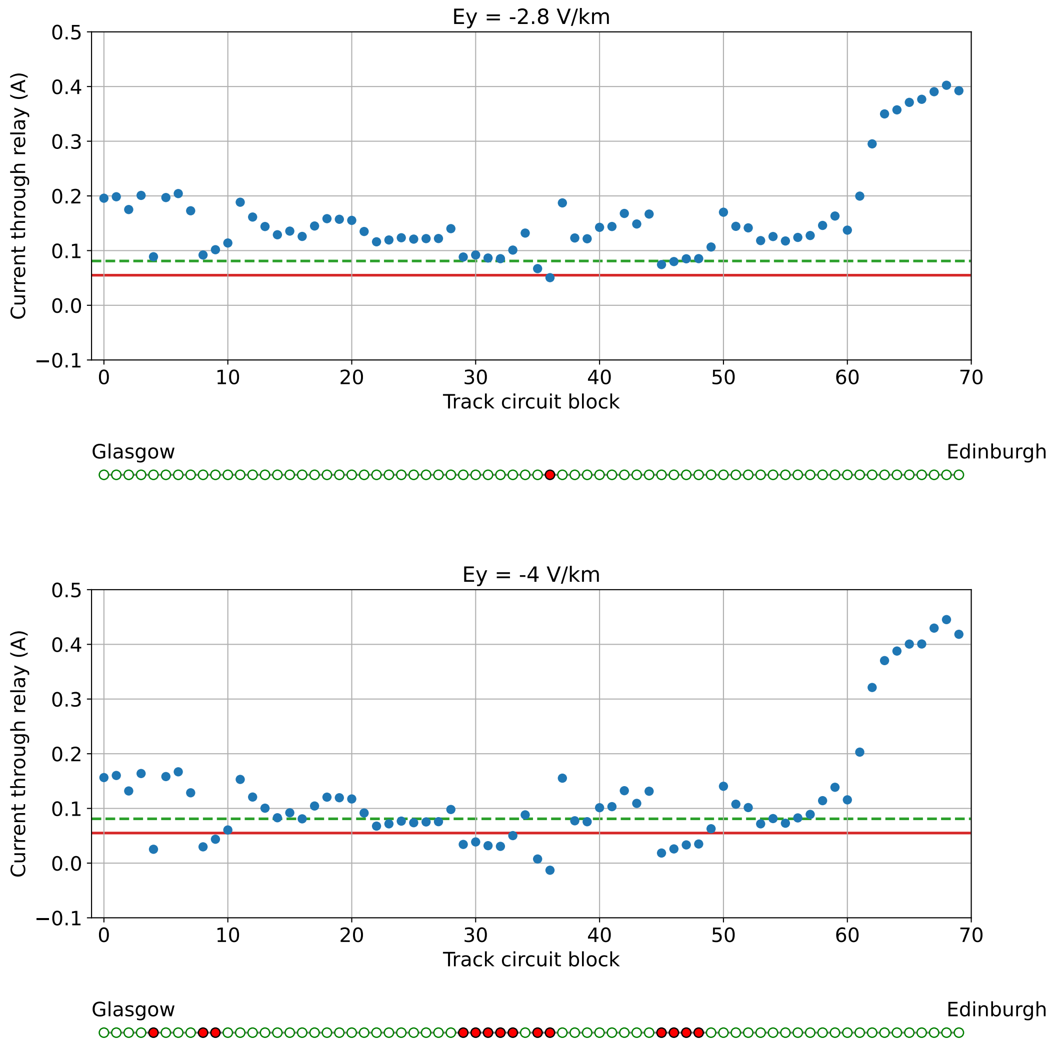


**Figure 11.** In the absence of a train, for each of the geoelectric fields applied: the current through each of the 75 track circuit relays between Glasgow and Edinburgh. The blue dots indicate the current of each relay, the red (solid) line shows the threshold below which the track circuit would de-energise and display an incorrect signal, and the green (dashed) line shows the threshold the current would need to rise above to re-energise if de-energised. Below each plot is a schematic view of each signal and whether it is operating correctly, an unfilled green dot means normal operation and a filled red dot indicates a misoperation. In this case, there are signal misoperations at $E_y = -2.8\,\mathrm{V\,km^{-1}}$ (1 misoperation) and $E_y = -4\,\mathrm{V\,km^{-1}}$ (14 misoperations).

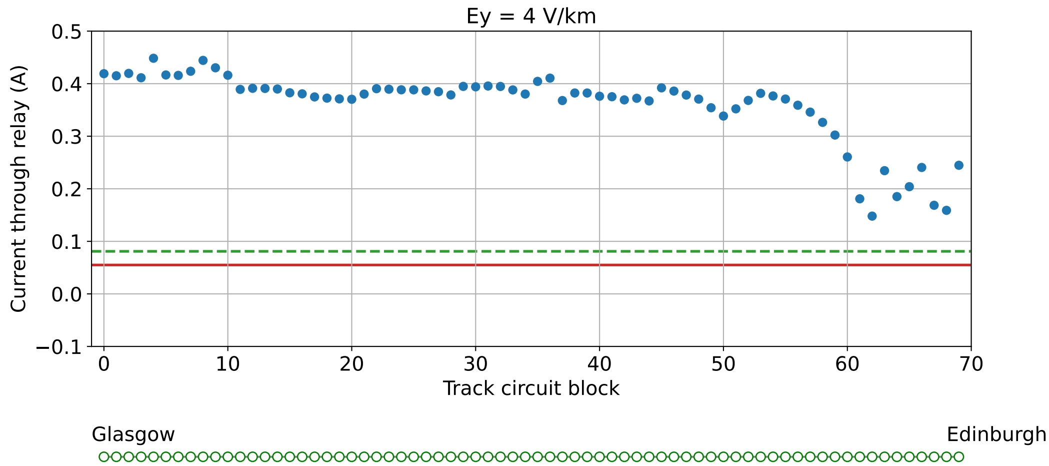


**Figure 12.** In the absence of a train, for each of the geoelectric fields applied: the current through each of the 75 track circuit relays between Glasgow and Edinburgh. The blue dots indicate the current of each relay, the red (solid) line shows the threshold below which the track circuit would de-energise and display an incorrect signal, and the green (dashed) line shows the threshold the current would need to rise above to re-energise if de-energised. Below each plot is a schematic view of each signal and whether it is operating correctly, an unfilled green dot means normal operation and a filled red dot indicates a misoperation. In this case, there are no signal misoperations at $E_y = 4\,\mathrm{V\,km^{-1}}$.

freight. The Glasgow to Edinburgh via Falkirk line was chosen for its east-west orientation and due to it being a connection between two major cities.

The model showed that the potential difference across track circuit relays near to the ends of the line can vary greatly from those in the centre even if they have identical properties and parameters. This means that the susceptibility of a track circuit block to induced currents cannot simply be determined from its length and orientation (i.e., alignment to the direction of the electric field). However, we have also shown that those assumptions are valid when studying sections of a longer line that are not near the ends of the traction rail.

The range of electric field values used in this analysis ($\pm 4\,\mathrm{V\,km^{-1}}$) is based on the electric field magnitude that caused signalling systems to misoperate in Sweden during a geomagnetic storm in July 1982 (Wik et al., 2009), where a value of 4-5 $\mathrm{V\,km^{-1}}$ was estimated. It was demonstrated that the two UK lines studied would have experienced signal misoperations if subjected to a geoelectric field of this magnitude. Comparing the electric field values at which signal misoperations begin to occur with estimates of electric fields across the UK for different timescales by Beggan et al. (2013), the value is equivalent to an event that could occur once every 30 years. Electric fields in the UK estimated for a 1 in 100-year extreme geomagnetic field by Beggan et al. (2013) were demonstrated to cause significant disruptions to the two lines studied, with a large number of signal misoperations occurring.

While the electrical characteristics of the rails used in this study are the conventional values given in Network Rail standards, there can be variation in these parameters. For example, the leakage from the rails to the ground is affected by the weather, increasing in wetter conditions and decreasing in drier conditions. The model was rerun using the range of leakage from the rails to the ground from Network Rail standard

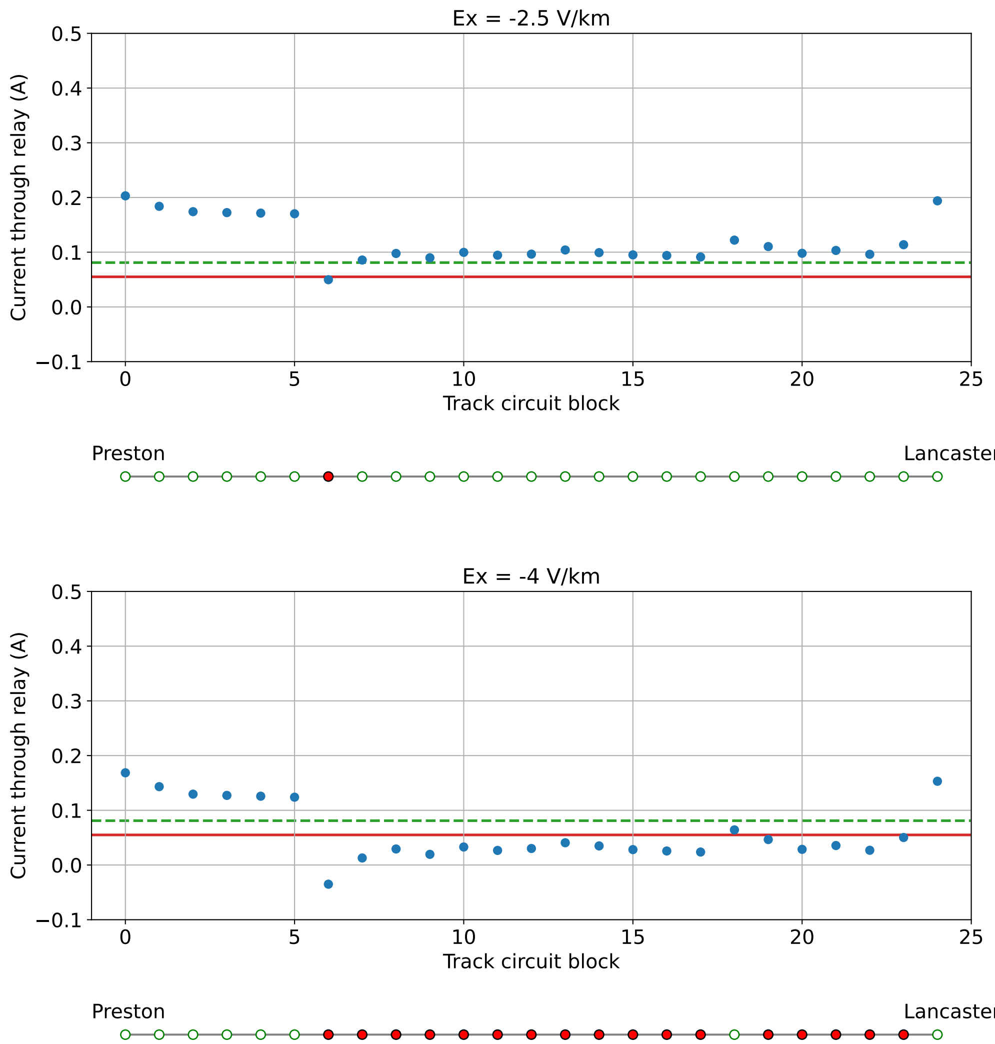


**Figure 13.** In the absence of a train, for each of the geoelectric fields applied: the current through each of the 25 track circuit relays between Preston and Lancaster with various geoelectric field strengths applied. The blue dots indicate the current of each relay, the red (solid) line shows the threshold below which the track circuit would de-energise and display an incorrect signal, and the green (dashed) line shows the threshold the current would need to rise above to re-energise if de-energised. Below each plot is a schematic view of each signal and whether it is operating correctly, an unfilled green dot means normal operation and a filled red dot indicates a misoperation. In this case, there are signal misoperations at $E_x = -2.5\,\mathrm{V\,km^{-1}}$ (1 misoperation) and $E_x = -4\,\mathrm{V\,km^{-1}}$ (17 misoperations).

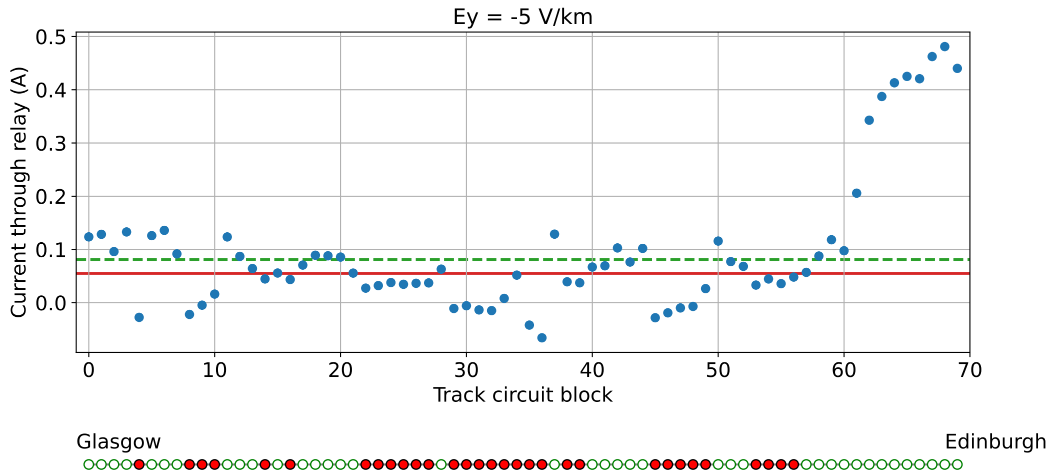


**Figure 14.** In the absence of a train, for each of the geoelectric fields applied: the current through each of the 75 track circuit relays between Glasgow and Edinburgh. The blue dots indicate the current of each relay, the red (solid) line shows the threshold below which the track circuit would de-energise and display an incorrect signal, and the green (dashed) line shows the threshold the current would need to rise above to re-energise if de-energised. Below each plot is a schematic view of each signal and whether it is operating correctly, an unfilled green dot means normal operation and a filled red dot indicates a misoperation. In this case, almost half of the signals are showing misoperations.

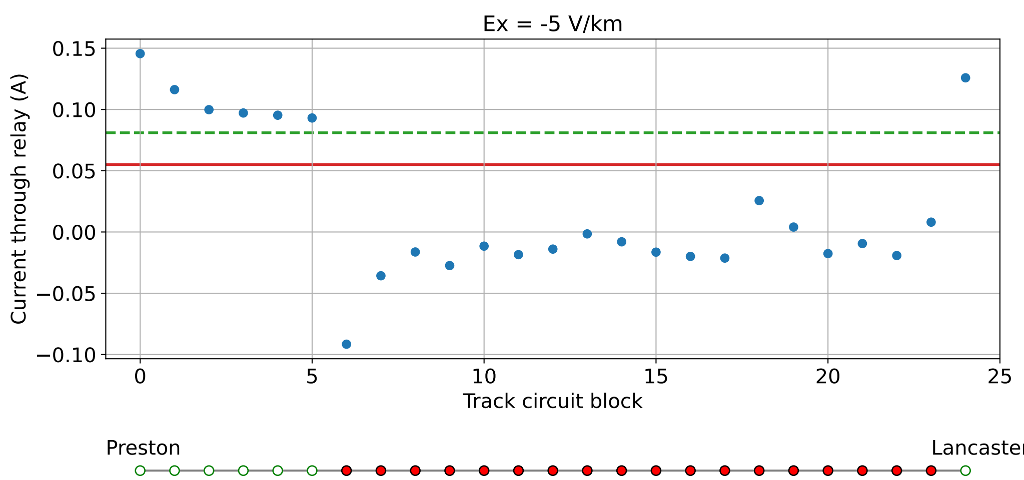


**Figure 15.** In the absence of a train, for each of the geoelectric fields applied: the current through each of the 25 track circuit relays between Preston and Lancaster with various geoelectric field strengths applied. The blue dots indicate the current of each relay, the red (solid) line shows the threshold below which the track circuit would de-energise and display an incorrect signal, and the green (dashed) line shows the threshold the current would need to rise above to re-energise if de-energised. Below each plot is a schematic view of each signal and whether it is operating correctly, an unfilled green dot means normal operation and a filled red dot indicates a misoperation. In this case, almost all of the signals are showing misoperations.

NR/GN/ELP/27312 (2006), and the results are as follows. It was found that when the leakage to the ground was maximised ($0.4\,\mathrm{S\,km^{-1}}$ for the signalling rail and $2\,\mathrm{S\,km^{-1}}$ for the traction rail), the threshold electric field values at which signal misoperations begin to occur was lowered for both Glasgow to Edinburgh and Preston to Lancaster to $-0.9\,\mathrm{V\,km^{-1}}$ and $-0.7\,\mathrm{V\,km^{-1}}$ respectively. When the leakage to the ground was minimised ($0.025\,\mathrm{S\,km^{-1}}$ for the signalling rail and $1.53\,\mathrm{S\,km^{-1}}$ for the traction rail), the threshold electric field values at which signal misoperations begin to occur was raised for both Glasgow to Edinburgh and Preston to Lancaster to $-4.3\,\mathrm{V\,km^{-1}}$ and $-4\,\mathrm{V\,km^{-1}}$ respectively. This means we are more likely to see signal misoperations on days that are wetter than average and vice versa. We also tested the impact of altering the rail resistance, but it was found that varying either or both of the rail's resistance values did not result in a significant change to the results.

It was shown that signal misoperations only occurred when the applied electric field was negative (i.e. opposite to the general direction of travel). This was due to the field being orientated such that the induced currents mostly contributed towards de-energising the relays, flowing across the relay in a direction opposite to the current provided by the track circuit power supply. When the applied electric field was positive, the relays became more energised. This was the general case for most of the track circuit blocks, but if the model includes the entirety of the traction rail, the currents across the relays in blocks near a characteristic crossover point become less sensitive to the changes in the electric field. In blocks beyond the crossover point, the direction of current across the relays will be reversed, becoming increasingly energised with a more negative electric field. In the case of the Glasgow to Edinburgh line, the blocks beyond the crossover point do not de-energise sufficiently to cause a misoperation even when the electric field is at the maximum positive value of the range used in this study, this is mainly due to the length of those blocks, which happen to be the shortest ones on the line as they are approaching the terminal station in a large city. It is worth noting that this paper only considers one direction of each line studied, depending on the orientation and layout of the track circuits, positive electric fields could cause signal misoperations in other cases, e.g., for the opposite direction of travel.

In this study, we have focused on geoelectric fields of constant direction and magnitude, when in reality they typically vary in intensity and direction over time. We note that the impact of time-varying fields will need to be considered in future work. For example, the duration over which geoelectric fields must maintain a given strength and/or orientation to cause a misoperation remains unclear. In such cases, the characteristic response times of various types of track circuits to current changes will also need to be examined. Furthermore, given the diverging/converging current flows shown in Figure 7, the possibility of charge build-up (that may work to oppose the geoelectric field) should be explored.

The impact of space weather on railway signalling is but one aspect of a multifaceted system that is intrinsically connected. Alongside signalling systems, the operation of a railway network also relies upon many interdependent systems such as power transmission, communication and Global Navigation Satellite Systems (GNSS), all of which are susceptible to the effects of space weather (Hapgood et al., 2021). The UK report on rail resilience to space weather Darch et al. (2014) states: "Accidents are rarely caused by a single failure; compound effects from multiple impacts are likely to create a problem" (p.5). Considering the delays that the railway network could be subjected to in the case of extensive signalling misoperations, passengers could potentially be trapped on a stationary train for extended periods. This is especially likely if other interdependent systems are also affected. The onboard air-conditioning and toilet systems are unable to continue operating for long periods without external power sources, subjecting passengers to uncomfortable and potentially harmful conditions. In this eventuality, if passengers were to take it upon themselves to leave the train unaided, then they would be subjected to severe risk due to currents flowing in the rails, trains on adjacent lines and a plethora of other hazards from walking unattended along a potentially remote section of track.

The simplification of not including trains in the model was necessary at this initial stage of model development. This also aided in getting an overview of the fundamental principles of how induced currents affect the rails and infrastructure without other sources of interference. While this setup was ideal for analysing the 'right side failures' that occur when trains are absent from track circuit blocks, a study into the more hazardous case of 'wrong side failures' will be greatly beneficial to furthering our understanding of geomagnetic interference in railway signalling systems. We consider that to be a natural next step for this research.

## 6 Conclusion

This study presents the most realistic model of geomagnetic interference in DC signalling systems on AC-electrified railway lines to date. Built upon the techniques detailed in Boteler (2021) we have modelled two sections of the UK railway network, the north-south orientated Preston to Lancaster section of the West Coast Main Line and the east-west orientated Glasgow to Edinburgh via Falkirk line.

Comparing these two sections, the model showed that the extent to which induced currents can affect track circuit relays depends heavily on whether the section studied includes the ends of the traction rail or whether it is part of a longer line. When considering the impact on relays in the centre of a line it can be seen that block length is a first-order indicator of current across the relays. The angular difference between the rail orientation and the electric field direction is also a factor, with blocks aligned parallel to the electric field having the largest currents induced along them. There are also further subtle effects such as the lengths of blocks adjacent to a given track circuit block which can affect the overall voltage profile.

Uniform electric fields of magnitude comparable to those reported in Sweden (Wik et al., 2009) were applied to the track sections in our model. The threshold electric field that generated sufficiently strong GICs to cause relay de-energisation in the Glasgow to Edinburgh line was $-2.8\,\mathrm{V\,km^{-1}}$. For the Preston to Lancaster section of the West Coast Main Line, the threshold electric field that caused signal misoperations was $-2.5\,\mathrm{V\,km^{-1}}$. These values are equivalent to those generated by events that could occur approximately once every 30 years. When electric field was strengthened to $-4\,\mathrm{V\,km^{-1}}$, many misoperations occurred on both lines. For the Glasgow to Edinburgh line, in the blocks after the crossover point where the polarity of the potential difference is reversed, an electric field of $4\,\mathrm{V\,km^{-1}}$ was insufficient to cause any misoperations, mainly due to the short length of those blocks.

Applying a 1 in 100-year extreme geoelectric field, estimated to be $-5\,\mathrm{V\,km^{-1}}$, the GICs generated were strong enough to severely affect the signals in the Glasgow to Edinburgh and Preston to Lancaster lines. In this case, nearly all of the signals in both sections would misoperate, leading to significant operational impacts.

## 7 Open Research

Network Rail standard documents can be obtained from `https://global.ihs.com/csf_home.cfm?&csf=NR`. The magnetic storm data are accessible at `https://www.intermagnet.org/data-donnee/download-eng.php`. The OpenStreetMap railway geometry data and the processed data using information from Traksy (https://traksy.uk/live) and the Network Rail Sectional Appendix are available at DOI: 10.17635/lancaster/researchdata/580.

**Acknowledgments**

The authors thank Ian Flintoft and Les McCormack at Atkins, a member of the SNC-Lavalin Group, who provided invaluable support and guidance on obtaining current UK relevant railway data. They also thank Brian Haddock of Network Rail for aiding in the acquisition of UK railway standards. They thank Ciaran Beggan of the NERC British Geological Survey for helpful discussions. The results presented in this paper rely on data collected at magnetic observatories. We thank the national institutes that support them and INTERMAGNET for promoting high standards of magnetic observatory practice. CJP was supported in the interdisciplinary research by STFC studentship [ST/V506795/1]. JAW was supported by the NERC Highlight Topic "Space Weather Impacts on Ground-based Systems (SWIGS)" award [NE/P016715/1].

## References

Alm, E. (1956). Measures against geomagnetic disturbances in the entire dc track circuit for automatic signalling systems, original publication (in swedish) appendix 5f, betänkande: angående det tekniska utförandet av signalanläggningar vid statens järnvägar, 1956. Translation (in English), June 2020. *Infrastructure Resilience Risk Reporter*, *1*, 28-51. Retrieved from `https://carleton.ca/irrg/journal/`

Beggan, C. D., Beamish, D., Richards, A., Kelly, G. S., & Alan, A. W. (2013, 7). Prediction of extreme geomagnetically induced currents in the UK high-voltage network. *Space Weather*, *11*, 407-419. doi: 10.1002/swe.20065

Boteler, D. H. (1997). Distributed-source transmission line theory for electromagnetic induction studies. *Proceedings of the 1997 Zurich EMC Symposium*, 401–408.

Boteler, D. H. (2013). A new versatile method for modelling geomagnetic induction in pipelines. *Geophysical Journal International*, *193*, 98-109. doi: 10.1093/gji/ggs113

Boteler, D. H. (2014). Methodology for simulation of geomagnetically induced currents in power systems. *Journal of Space Weather and Space Climate*, *4*. doi: 10.1051/swsc/2014018

Boteler, D. H. (2021). Modeling geomagnetic interference on railway signaling track circuits. *Space Weather*, *19*. doi: 10.1029/2020SW002609

Boteler, D. H., & Trichtchenko, L. (2015). Telluric influence on pipelines. In R. W. Revie (Ed.), *Oil and gas pipelines: Integrity and safety handbook* (p. 275-288). John Wiley and Sons, Inc. doi: 10.1002/9781119019213.ch21

*British steel: Rail product range* (Tech. Rep.). (2020). PO Box 1, Brigg Road, Scunthorpe, North Lincolnshire, DN16 1BP, United Kingdom: British Steel.

Cabinet Office. (2012). *National risk register of civil emergencies.* 22 Whitehall, London, SW1A 2WH.

Darch, G., McCormack, L., Hayes, D., Tomlinson, J., Hooper, P., Williams, R., ... Tyndall, M. (2014). *Rail resilience to space weather final phase 1 report department for transport* (Tech. Rep.). Western House (Block B), Peterborough Business Park, Lynch Wood, Peterborough, PE2 6FZ: Atkins Limited.

Department for Transport. (2015). *Supplement to the october 2013 strategic case for hs2 technical annex: Demand and capacity pressures on the west coast main line.* Great Minster House, 33 Horseferry Road, London, SW1P 4DR.

Eroshenko, E. A., Belov, A. V., Boteler, D., Gaidash, S. P., Lobkov, S. L., Pirjola, R., & Trichtchenko, L. (2010). Effects of strong geomagnetic storms on northern railways in russia. *Advances in Space Research*, *46*, 1102-1110. doi: 10.1016/j.asr.2010.05.017

Hapgood, M., Angling, M. J., Attrill, G., Bisi, M., Cannon, P. S., Dyer, C., ... Willis, M. (2021). Development of space weather reasonable worst-case scenarios for the uk national risk assessment. *Space Weather*, *19*. doi:

10.1029/2020SW002593

Kasinskii, V. V., Ptitsyna, N. G., Lyahov, N. N., Tyasto, M. I., Villoresi, G., & Iucci, N. (2007). Effect of geomagnetic disturbances on the operation of railroad automated mechanisms and telemechanics. *Geomagnetism and Aeronomy*, *47*, 676-680. doi: 10.1134/S0016793207050179

Keenor, G. (2021). *Overhead line electrification for railways - 6th-edition.* Keenor. Retrieved from https://ocs4rail.com/downloads/

Krausmann, E., Andersson, E., Russell, T., & Murtagh, W. (2015). *Space weather and rail: Findings and outlook* (Tech. Rep.). Joint Research Centre, Via E. Fermi 2749, 21027 Ispra (VA), Italy: European Commission. Retrieved from https://ec.europa.eu/jrc doi: 10.2788/211456

Lejdström, B., & Svensson, S. (1956). Calculation of geomagnetic interference voltages in track circuits, original publication (in swedish) appendix 6, betänkande: angående det tekniska utförandet av signalanläggningar vid statens järnvägar, 1956. Translation (in English) June 2020. *Infrastructure Resilience Risk Reporter*, *1*, 28-51. Retrieved from https://carleton.ca/irrg/journal/

Lewis, Z. M., Wild, J. A., Allcock, M., & Walach, M. T. (2022). Assessing the impact of weak and moderate geomagnetic storms on UK power station transformers. *Space Weather*, *20*. doi: 10.1029/2021SW003021

Liu, L., Ge, X., Zong, W., Zhou, Y., & Liu, M. (2016). Analysis of the monitoring data of geomagnetic storm interference in the electrification system of a high-speed railway. *Space Weather*, *14*, 754-763. doi: 10.1002/2016SW001411

Mariscotti, A. (2020). Impact of rail impedance intrinsic variability on railway system operation, emc and safety. *International Journal of Electrical and Computer Engineering*, *9*. doi: 10.11591/ijece.v9i4.ppxx-xx

NR/BR/867. (1990). *Specification for ac immune dc track feed units* (Tech. Rep.). 40 Melton Street, London, NW1 2EE: Network Rail.

NR/BR/939A. (1971). *Specification for miniature tractive armature ac immune dc neutral track relay, plug-in type for railway signalling purposes* (Tech. Rep.). 40 Melton Street, London, NW1 2EE: Network Rail.

NR/GN/ELP/27312. (2006). *Impedances of 25 kv a.c. overhead lines for classic system* (Tech. Rep.). 40 Melton Street, London, NW1 2EE: Network Rail.

NR/PS/SIG/11755. (2000). *Dc track circuits (formerly rt/e/ps/11755)* (Tech. Rep.). 40 Melton Street, London, NW1 2EE: Network Rail.

NR/SP/SIG/50004. (2006). *Methodology for the demonstration of electrical compatibility with dc (ac immune) track circuits* (Tech. Rep.). 40 Melton Street, London, NW1 2EE: Network Rail.

Pirjola, R. (1985). On currents induced in power transmission systems during geomagnetic variations. *IEEE Transactions on Power Apparatus and Systems*, *PAS-104*, 2825-2831. doi: 10.1109/TPAS.1985.319126

Ptitsyna, N. G., Kasinskii, V. V., Villoresi, G., Lyahov, N. N., Dorman, L. I., & Iucci, N. (2008). Geomagnetic effects on mid-latitude railways: A statistical study of anomalies in the operation of signaling and train control equipment on the east-siberian railway. *Advances in Space Research*, *42*, 1510-1514. doi: 10.1016/j.asr.2007.10.015

Pulkkinen, A., Viljanen, A., Pajunpää, K., & Pirjola, R. (2002). Recordings and occurrence of geomagnetically induced currents in the Finnish natural gas pipeline network. *Applied Geophysics*, *48*.

Wik, M., Pirjola, R., Lundstedt, H., Viljanen, A., Wintoft, P., & Pulkkinen, A. (2009). Space weather events in july 1982 and october 2003 and the effects of geomagnetically induced currents on swedish technical systems. *Annales Geophysicae*, *27*, 1775-1787.